JOURNAL OF COMPUTATIONAL PHYSICS **133,** 102–112 (1997)
ARTICLE NO. CP975657

Analysis of the Turkel–Zwas Scheme for the Two-Dimensional Shallow Water Equations in Spherical Coordinates

B. Neta,*[,1,2] F. X. Giraldo,*[,3] and I. M. Navon†

*Department of Mathematics, Naval Postgraduate School, Monterey, California 93943; and †Department of Mathematics and Supercomputer Computations Research Institute, Florida State University, Tallahassee, Florida 32306

Received December 5, 1995; revised November 26, 1996

A linear analysis of the shallow water equations in spherical coordinates for the Turkel–Zwas (T–Z) explicit large time-step scheme is presented. This paper complements the results of Schoenstadt, Neta and Navon, and others in 1-D, and of Neta and DeVito in 2-D, but applied to the spherical coordinate case of the T–Z scheme. This coordinate system is more realistic in meteorology and more complicated to analyze, since the coefficients are no longer constant. The analysis suggests that the T–Z scheme must be staggered in a certain way in order to get eigenvalues and eigenfunctions approaching those of the continuous case. The importance of such an analysis is the fact that it is also valid for nonconstant coefficients and thereby applicable to any numerical scheme. Numerical experiments comparing the original (unstaggered) and staggered versions of the T–Z scheme are presented. These experiments corroborate the analysis by showing the improvements in accuracy gained by staggering the Turkel–Zwas scheme.

1. INTRODUCTION

The transfer function was first introduced in electrical engineering by Stremler [7]. It is different from Fourier analysis since it gives information about amplitude distortion and not just phase. Schoenstadt [2] has applied the idea to comparison of various schemes for the one-dimensional shallow water system. Neta and Navon [3] extended the results to include the Turkel–Zwas [1] explicit large time-step scheme on a limited-area domain for the shallow water equations. Steppeler [8, 9] analyzed some hybrid methods. Neta and DeVito [4] extended Schoenstadt's results to the two-dimensional case. Neta [10] has extended the transfer function analysis to the two-dimensional Turkel–Zwas explicit large time-step finite difference scheme in a Cartesian coordinate system. Song and Tang [13] have used the Laplace transform instead of the Fourier transform to analyze the unstaggered as well as the staggered Turkel–Zwas scheme.

In this paper we extend the linear transfer function analysis to the two-dimensional shallow water equations in spherical coordinates for the Turkel–Zwas discretization. Actually, we show how to obtain the modal expansion for the shallow water equations in spherical coordinates and for the Turkel–Zwas discretization of these equations. At this point, we should comment on the choice of the method. Computationally efficient and accurate schemes for the numerical solution of the shallow water equations are of crucial importance in atmospheric and oceanographic models. Two different approaches have been taken, both of them dealing with the different time scales of advective (Rossby) waves and gravity inertia waves separately. The first of these was the split-explicit and semi-implicit schemes. The Turkel–Zwas scheme takes a different view by proposing a space (rather than time) splitting approach. This is based on the fact that the fast gravity inertia waves which restrict the time step contain only a small fraction of the total available energy and therefore can be calculated with a lower accuracy on a coarse grid. The Rossby waves which contain most of the energy are calculated on the finer mesh. When the ratio of the coarse and fine grids is an integer $p > 1$, one can use time steps nearly p times larger than those allowed by the usual explicit scheme. The CFL condition for the Turkel–Zwas scheme on a rectangular domain can be found in Turkel and Zwas [1] and Song and Tang [13]. For spherical coordinated, the CFL condition is given in Navon and deVilliers [5]:

$$\Delta t \le \frac{a \cos\theta}{\sqrt{gH}} \frac{p\Delta\lambda}{\sin pk\Delta\lambda}.$$

The importance of this explicit scheme is also in parallelization. It is always easier to use an explicit scheme on parallel computers and certainly these modifications and the analysis will encourage the development of a parallel Turkel–Zwas scheme.

In Section 2 we present the modal expansion for linearized shallow water equations in spherical coordinates with no mean flow. We start (Subsection 2.1) by obtaining the

[1] Part of this research was conducted while the author was visiting the Department of Mathematics at the Technion, Haifa, Israel.

[2] To whom correspondence should be addressed.

[3] Current address: Naval Research Laboratory, Monterey, California 93940.

0021-9991/97 $25.00

linearization of the shallow water equations on the sphere. Then (Subsection 2.2) we describe the modal expansion for the linearized system as obtained by Longuet-Higgins [12]. In Section 3 we present the modal expansion for the linearized shallow water equations in spherical coordinates discretized using the Turkel–Zwas finite difference scheme. We start this section by describing the Turkel–Zwas scheme (Subsection 3.1). The modal expansion is given in Subsection 3.2. As a result of this analysis, we conclude that certain staggering is necessary. A modified staggered method, different from those suggested by Song and Tang [13], is given in Section 4. Again this section is subdivided into two subsections. The first subsection describes the staggered discretization and the second gives the modal expansion. In Section 5 we compare the modal expansion for the discrete and continuous cases. In Section 6 we present the numerical results of this study showing the benefits gained by staggering the Turkel–Zwas scheme for the shallow water equations, and in Section 7 we give the concluding remarks.

2. SHALLOW WATER EQUATIONS

2.1. *Linearization*

The shallow water equations in spherical coordinates are given by

$$\frac{\partial u}{\partial t} + \frac{1}{a\cos\theta}\left[u\frac{\partial u}{\partial \lambda} + v\cos\theta\frac{\partial u}{\partial \theta}\right] - \left(f + \frac{u}{a}\tan\theta\right)v + \frac{g}{a\cos\theta}\frac{\partial h}{\partial \lambda} = 0 \tag{1}$$

$$\frac{\partial v}{\partial t} + \frac{1}{a\cos\theta}\left[u\frac{\partial v}{\partial \lambda} + v\cos\theta\frac{\partial v}{\partial \theta}\right] + \left(f + \frac{u}{a}\tan\theta\right)u + \frac{g}{a}\frac{\partial h}{\partial \theta} = 0 \tag{2}$$

$$\frac{\partial h}{\partial t} + \frac{1}{a\cos\theta}\left[\frac{\partial}{\partial \lambda}(hu) + \frac{\partial}{\partial \theta}(hv\cos\theta)\right] = 0. \tag{3}$$

Here, f is the Coriolis parameter given by

$$f = 2\Omega\sin\theta, \tag{4}$$

where Ω is the angular speed of the rotation of the earth, h is the height of the homogeneous atmosphere, u and v are the zonal and meridional wind components, respectively, θ and λ are the latitudinal and longitudinal directions, respectively, a is the radius of the earth, and g is the gravitational constant.

The two-dimensional linearized shallow water equations (LSW) with no mean flow in spherical coordinates are

$$\frac{\partial u}{\partial t} - fv + \frac{g}{a\cos\theta}\frac{\partial h}{\partial \lambda} = 0 \tag{5}$$

$$\frac{\partial v}{\partial t} + fu + \frac{g}{a}\frac{\partial h}{\partial \theta} = 0 \tag{6}$$

$$\frac{\partial h}{\partial t} + \frac{H}{a\cos\theta}\left(\frac{\partial u}{\partial \lambda} + \frac{\partial}{\partial \theta}(v\cos\theta)\right) = 0, \tag{7}$$

where H is the mean height of the surface and h is the perturbation. In the next subsection we describe the modal expansion given by Longuet-Higgins [12].

2.2. *Modal Expansion to the LSW (Longuet-Higgins)*

For the case of interest here, f is *not* constant. *We follow the discussion in Longuet-Higgins* [12] on Laplace's tidal equations, which are (5)–(7). We should remark here that the variable θ in Longuet-Higgins [12] is $\pi/2 - \theta$. We seek periodic solutions to (5)–(7) which are proportional to $e^{i(m\lambda - ct)}$, where m is a nonnegative integer and c a constant nonzero frequency. Substituting such an exponential in (5)–(7), we get im instead of $\partial/\partial\lambda$, and $-ic$ instead of $\partial/\partial t$.

Longuet-Higgins [12] introduced functions analogous to the velocity potential (Φ) and stream function (Ψ), such that

$$u = \frac{1}{\cos\theta}\frac{\partial \Phi}{\partial \lambda} + \frac{\partial \Psi}{\partial \theta} \tag{8}$$

$$v = \frac{\partial \Phi}{\partial \theta} - \frac{1}{\cos\theta}\frac{\partial \Psi}{\partial \lambda}. \tag{9}$$

Then $\nabla^2\Phi$, $\nabla^2\Psi$ are the divergence and vorticity, where ∇^2 denotes the horizontal Laplacian operator,

$$\nabla^2 = \frac{1}{\cos\theta}\left[\frac{\partial}{\partial \theta}\left(\cos\theta\frac{\partial}{\partial \theta}\right) + \frac{1}{\cos\theta}\frac{\partial^2}{\partial \lambda^2}\right]. \tag{10}$$

Longuet-Higgins has shown that

$$\frac{\partial}{\partial t}\nabla^2\Phi + 2\Omega\sin\theta\nabla^2\Psi + 2\Omega\cos\theta u + \frac{g}{a}\nabla^2 h = 0 \tag{11}$$

$$\frac{\partial}{\partial t}\nabla^2\Psi - 2\Omega\sin\theta\nabla^2\Phi - 2\Omega\cos\theta v = 0. \tag{12}$$

Equation (7) can also be written

$$\frac{\partial h}{\partial t} + \frac{H}{a}\nabla^2\Phi = 0. \tag{13}$$

We substitute for u and v from (8) and (9) to get

$$\left(\frac{\partial}{\partial t}\nabla^2 + 2\Omega\frac{\partial}{\partial\lambda}\right)\Phi + 2\Omega\left(\sin\theta\nabla^2 + \cos\theta\frac{\partial}{\partial\lambda}\right)\Psi = -\frac{g}{a}\nabla^2 h \quad (14)$$

$$\left(\frac{\partial}{\partial t}\nabla^2 + 2\Omega\frac{\partial}{\partial\lambda}\right)\Psi - 2\Omega\left(\sin\theta\nabla^2 + \cos\theta\frac{\partial}{\partial\lambda}\right)\Phi = 0. \quad (15)$$

We seek solutions to these equations (13)–(15) proportional to $e^{i(m\lambda - ct)}$, where m is a nonnegative integer and c denotes the radian frequency. For convenience we use the operator D as

$$D = (1-\mu^2)\frac{\partial}{\partial\mu}, \quad (16)$$

where

$$\mu = \sin\theta. \quad (17)$$

Then Eqs. (13)–(15) become

$$(\Lambda\nabla^2 - m)\Phi + (\mu\nabla^2 + D)\, i\Psi = -\frac{ig}{2\Omega}\nabla^2 h \quad (18)$$

$$(\Lambda\nabla^2 - m)\, i\Psi + (\mu\nabla^2 + D)\Phi = 0 \quad (19)$$

$$ich = \frac{H}{a}\nabla^2\Phi, \quad (20)$$

where now

$$\nabla^2 \equiv \frac{d}{d\mu}\left[(1-\mu^2)\frac{d}{d\mu}\right] - \frac{m^2}{1-\mu^2} \quad (21)$$

and

$$\Lambda = \frac{c}{2\Omega}. \quad (22)$$

Upon eliminating h from (18) and (20) we get

$$\left(\Lambda\nabla^2 - m + \frac{a^2}{\varepsilon\Lambda}\nabla^4\right)\Phi + (\mu\nabla^2 + D)\, i\Psi = 0, \quad (23)$$

where

$$\varepsilon = \frac{4\Omega^2 a^2}{gH}. \quad (24)$$

In the next section, we follow a similar derivation for the semidiscretization given by the Turkel–Zwas scheme. We will show how Eqs. (18)–(20) and (23) will be affected by the discretization and prove that staggering is necessary. It should be noted that the idea can be applied to *any* numerical (semidiscrete) scheme.

3. UNSTAGGERED TURKEL–ZWAS SCHEME

3.1. *Discretization*

Given a constant α, $0 < \alpha \le 1$, the Turkel–Zwas scheme for the nonlinear shallow water equations in spherical coordinates takes the form

$$\begin{aligned} u_{k,j}^{l+1} = u_{k,j}^{l-1} &- \sigma\left[\frac{u_{k,j}^l}{\cos\theta_j}(u_{k+1,j}^l - u_{k-1,j}^l) + v_{k,j}^l(u_{k,j+1}^l - u_{k,j-1}^l)\right. \\ &\left. + \frac{g}{p\cos\theta_j}(h_{k+p,j}^l - h_{k-p,j}^l)\right] \\ &+ 2\Delta t\left[(1-\alpha)\left(f_j + \frac{u_{k,j}^l}{a}\tan\theta_j\right)v_{k,j}^l\right. \\ &+ \frac{\alpha}{2}\left(f_j + \frac{u_{k+p,j}^l}{a}\tan\theta_j\right)v_{k+p,j}^l \\ &\left. + \frac{\alpha}{2}\left(f_j + \frac{u_{k-p,j}^l}{a}\tan\theta_j\right)v_{k-p,j}^l\right] \end{aligned} \quad (25)$$

$$\begin{aligned} v_{k,j}^{l+1} = v_{k,j}^{l-1} &- \sigma\left[\frac{u_{k,j}^l}{\cos\theta_j}\left(v_{k+1,j}^l - v_{k-1,j}^l\right) + v_{k,j}^l(v_{k,j+1}^l - v_{k,j-1}^l)\right. \\ &\left. + \frac{g}{q}(h_{k,j+q}^l - h_{k,j-q}^l)\right] \\ &- 2\Delta t\left[(1-\alpha)\left(f_j + \frac{u_{k,j}^l}{a}\tan\theta_j\right)u_{k,j}^l\right. \\ &+ \frac{\alpha}{2}\left(f_{j+q} + \frac{u_{k,j+q}^l}{a}\tan\theta_{j+q}\right)u_{k,j+q}^l \\ &\left. + \frac{\alpha}{2}\left(f_{j-q} + \frac{u_{k,j-q}^l}{a}\tan\theta_{j-q}\right)u_{k,j-q}^l\right] \end{aligned} \quad (26)$$

$$\begin{aligned} h_{k,j}^{l+1} = h_{k,j}^{l-1} &- \sigma\left\{\frac{u_{k,j}^l}{\cos\theta_j}(h_{k+1,j}^l - h_{k-1,j}^l) + v_{k,j}^l(h_{k,j+1}^l - h_{k,j-1}^l)\right. \\ &+ \frac{h_{k,j}^l}{\cos\theta_j}\left[(1-\alpha)(u_{k+p,j}^l - u_{k-p,j}^l)\right. \\ &\left.\left. + \frac{\alpha}{2}(u_{k+p,j+q}^l - u_{k-p,j+q}^l + u_{k+p,j-q}^l - u_{k-p,j-q}^l)\right]\frac{1}{p}\right. \\ &+ \frac{h_{k,j}^l}{\cos\theta_j}\left[(1-\alpha)(v_{k,j+q}^l\cos\theta_{j+q} - v_{k,j-q}^l\cos\theta_{j-q})\right. \end{aligned}$$

$$+\frac{\alpha}{2}(v^l_{k+p,j+q}\cos\theta_{j+q}-v^l_{k+p,j-q}\cos\theta_{j-q}$$

$$+v_{k-p,j+q}\cos\theta_{j+q}-v_{k-p,j-q}\cos\theta_{j-q})\Big]\frac{1}{q}\Big\}, \quad (27)$$

where

$$\sigma=\frac{\Delta t}{a\,\Delta\lambda}=\frac{\Delta t}{a\,\Delta\theta}. \quad (28)$$

We note that the λ, θ components of the pressure gradient and divergence terms are differenced over points $p\,\Delta\lambda$, $q\,\Delta\theta$ (respectively) away rather than nearest neighbors. In this way, the terms associated with the gravity waves (which carry little energy) can be approximated less accurately and thus a larger time step can be allowed. For $\alpha = 0$, Turkel and Zwas showed that there is a deterioration of accuracy for p larger than one. For $\alpha = \frac{1}{3}$ the geostrophic balance and the incompressibility condition are satisfied to a higher order in the Cartesian coordinate case (see Turkel and Zwas [1], Navon and de Villiers [5] and Navon and Yu [6]). For the spherical coordinates case, again Turkel and Zwas show that the choice $\alpha = \frac{1}{3}$ was necessary to preserve accuracy when p or q is greater than one.

The Turkel–Zwas scheme for the approximation of (5)–(7) can be written as

$$\left.\frac{\partial u}{\partial t}\right|_{k,j}=-\frac{1}{2a\Delta\lambda}\frac{g}{p\cos\theta_j}(h_{k+p,j}-h_{k-p,j})$$

$$+f_j\left[(1-\alpha)v_{k,j}+\frac{\alpha}{2}(v_{k+p,j}+v_{k-p,j})\right] \quad (29)$$

$$\left.\frac{\partial v}{\partial t}\right|_{k,j}=-\frac{1}{2a\Delta\theta}\frac{g}{q}(h_{k,j+q}-h_{k,j-q})$$

$$-\left[(1-\alpha)f_j u_{k,j}+\frac{\alpha}{2}(f_{j+q}u_{k,j+q}+f_{j-q}u_{k,j-q})\right] \quad (30)$$

$$\left.\frac{\partial h}{\partial t}\right|_{k,j}=-\frac{1}{2a}\frac{H}{\cos\theta_j}\Big[(1-\alpha)\Big(\frac{u_{k+p,j}-u_{k-p,j}}{p\,\Delta\lambda}$$

$$+\frac{v_{k,j+q}\cos\theta_{j+q}-v_{k,j-q}\cos\theta_{j-q}}{q\,\Delta\theta}\Big)$$

$$+\frac{\alpha}{2}\Big(\frac{u_{k+p,j+q}-u_{k-p,j+q}}{p\,\Delta\lambda}+\frac{u_{k+p,j-q}-u_{k-p,j-q}}{p\,\Delta\lambda}$$

$$+\frac{v_{k+p,j+q}\cos\theta_{j+q}-v_{k+p,j-q}\cos\theta_{j-q}}{q\,\Delta\theta}$$

$$+\frac{v_{k-p,j+q}\cos\theta_{j+q}-v_{k-p,j-q}\cos\theta_{j-q}}{q\,\Delta\theta}\Big)\Big]. \quad (31)$$

Note that there is a typographical error in Eq. (11a) of Turkel and Zwas [1], which is our Eq. (29). We have also modified (to get a symmetric approximation, as suggested by Neta [9] for a rectangular domain) the right hand side of (11c) in Turkel and Zwas [1], which is (31) here.

3.2. *Modal Expansion for the Discretized System*

We follow the method of Longuet-Higgins to formulate the discrete eigenvalue problem. Now, define two functions analogous to the velocity potential and stream function such that at each point

$$u_{kj}=\frac{1}{\cos\theta_j}\delta_p\Phi_{kj}+\delta_q\Psi_{kj} \quad (32)$$

$$v_{kj}=\delta_q\Phi_{kj}-\frac{1}{\cos\theta_j}\delta_p\Psi_{kj}, \quad (33)$$

which are the discrete analog of (8) and (9), where

$$\delta_p\Phi_{kj}=\frac{\Phi_{k+p/2\,j}-\Phi_{k-p/2\,j}}{p\,\Delta\lambda} \quad (34)$$

$$\delta_q\Phi_{kj}=\frac{\Phi_{k\,j+q/2}-\Phi_{k\,j-q/2}}{q\,\Delta\theta}. \quad (35)$$

It can be shown that $\nabla^2\Phi$ and $\nabla^2\Psi$ satisfy the discrete analog of (10); i.e.,

$$\nabla^2\Phi_{kj}=\frac{1}{\cos^2\theta_j}\delta_p^2\Phi_{kj}+\frac{1}{\cos\theta_j}\delta_q(\cos\theta_j\delta_q\Phi_{kj}), \quad (36)$$

and similarly for Ψ.

Now combine the right hand sides of Eqs. (29) and (30) in the following way:

$$\frac{1}{\cos\theta_j}\left[\frac{(29)k+p/2\,j^4-(29)k-p/2\,j}{p\,\Delta\lambda}\right.$$

$$\left.+\frac{(30)k\,j+q/2\cos\theta_{j+q/2}-(30)_{k\,j-q/2}\cos\theta_{j-q/2}}{q\,\Delta\theta}\right].$$

After a lengthy algebraic manipulation, one has to $O((q\,\Delta\theta)^2)$, which agrees with (11),

$$\frac{\partial}{\partial t}\nabla^2\Phi_{kj}+2\Omega\sin\theta_j\nabla^2\Psi_{kj}+2\Omega\cos\theta_j u_{kj}+\frac{g}{a}\nabla^2 h_{kj}=0. \quad (37)$$

Taking

[4] This means that we have to evaluate (29) at the point $k + p/2\,j$ instead of $k\,j$ and similarly for the other terms in this equation and the next.

$$\frac{1}{\cos\theta_j}\left[-\frac{(30)k+p/2\,j-(30)k-p/2\,j}{p\,\Delta\lambda}+\frac{(29)k\,j+q/2\cos\theta_{j+q/2}-(29)_{k\,j-q/2}\cos\theta_{j-q/2}}{q\,\Delta\theta}\right]$$

one has (note the similarity to (12))

$$\frac{\partial}{\partial t}\nabla^2\Psi_{kj}-2\Omega\sin\theta_j\nabla^2\Phi_{kj}-2\Omega\cos\theta_j v_{kj}=0. \quad (38)$$

Substituting u_{kj}, v_{kj} from (32) and (33) into (37) and (38) one obtains (similarly to (14) and (15))

$$\left(\frac{\partial}{\partial t}\nabla^2+2\Omega\delta_p\right)\Phi_{kj}+2\Omega\,(\sin\theta_j\nabla^2+\cos\theta_j\delta_q)\,\Psi_{kj}+\frac{g}{a}\nabla^2 h_{kj}=0 \quad (39)$$

$$\left(\frac{\partial}{\partial t}\nabla^2+2\Omega\delta_p\right)\Psi_{kj}-2\Omega\,(\sin\theta_j\nabla^2+\cos\theta_j\delta_q)\,\Phi_{kj}=0. \quad (40)$$

Equation (31) can also be written (to second order in $q\,\Delta\theta$)

$$\frac{\partial h_{kj}}{\partial t}=-\frac{H}{a}\left\{\frac{1}{\cos^2\theta_j}\delta_{2p}\delta_p\Phi_{k\,j}+\frac{1}{\cos\theta_j}\delta_{2q}(\cos\theta_j\delta_q\Phi_{k\,j})+\frac{1}{\cos\theta_j}(\delta_{2p}\delta_q-\delta_{2q}\delta_p)\Psi_{k\,j}\right\}. \quad (41)$$

Note that (41) is slightly different from (13). The first two terms would combine to $\nabla^2\Phi_{k\,j}$ if we had δ_p, δ_q instead of δ_{2p}, δ_{2q}, respectively. In this case, the third term would then vanish. It may be easier to rewrite (41) as

$$\frac{\partial h_{kj}}{\partial t}=-\frac{H}{a}\left\{\nabla^2\Phi_{kj}+\frac{1}{\cos^2\theta_j}(\delta_{2p}-\delta_p)\delta_p\Phi_{kj}+\frac{1}{\cos\theta_j}(\delta_{2q}-\delta_q)(\cos\theta_j\delta_q\Phi_{k\,j})+\frac{1}{\cos\theta_j}(\delta_{2p}\delta_q-\delta_{2q}\delta_p)\Psi_{k\,j}\right\}, \quad (42)$$

where the first term is now the same as (13) and the others represent the perturbation. *These other terms actually suggest that one should take* $u_{k\pm p/2\,j}$, $v_{k\,j\pm q/2}$ *in* (31), *i.e., staggering the variable h.*

4. STAGGERED TURKEL–ZWAS SCHEME

4.1. *Discretization*

As was shown in the previous section, it is necessary to stagger the grid. The staggered version of the Turkel–Zwas scheme takes the form

$$\begin{aligned}u^{l+1}_{k,j}=u^{l-1}_{k,j}-\sigma\Bigg[&\frac{u^l_{k,j}}{\cos\theta_j}(u^l_{k+1,j}-u^l_{k-1,j})+v^l_{k,j}(u^l_{k,j+1}-u^l_{k,j-1})\\&+\frac{2g}{p\cos\theta_j}(h^l_{k+p/2,j}-h^l_{k-p/2,j})\Bigg]\\&+2\Delta t\left[(1-\alpha)\left(f_j+\frac{u^l_{k,j}}{a}\tan\theta_j\right)v^l_{k,j}\right.\\&+\frac{\alpha}{2}\left(f_j+\frac{u^l_{k+p/2,j}}{a}\tan\theta_j\right)v^l_{k+p/2,j}\\&\left.+\frac{\alpha}{2}\left(f_j+\frac{u^l_{k-p/2,j}}{a}\tan\theta_j\right)v^l_{k-p/2,j}\right] \quad (43)\end{aligned}$$

$$\begin{aligned}v^{l+1}_{k,j}=v^{l-1}_{k,j}-\sigma\Bigg[&\frac{u^l_{k,j}}{\cos\theta_j}(v^l_{k+1,j}-v^l_{k-1,j})+v^l_{k,j}(v^l_{k,j+1}-v^l_{k,j-1})\\&+\frac{2g}{q}(h^l_{k,j+q/2}-h^l_{k,j-q/2})\Bigg]\\&-2\Delta t\left[(1-\alpha)\left(f_j+\frac{u^l_{k,j}}{a}\tan\theta_j\right)u^l_{k,j}\right.\\&+\frac{\alpha}{2}\left(f_{j+q/2}+\frac{u^l_{k,j+q/2}}{a}\tan\theta_{j+q/2}\right)u^l_{k,j+q/2}\\&\left.+\frac{\alpha}{2}\left(f_{j-q/2}+\frac{u^l_{k,j-q/2}}{a}\tan\theta_{j-q/2}\right)u^l_{k,j-q/2}\right] \quad (44)\end{aligned}$$

$$\begin{aligned}h^{l+1}_{k,j}=h^{l-1}_{k,j}-\sigma\Bigg\{&\frac{u^l_{k,j}}{\cos\theta_j}(h^l_{k+1,j}-h^l_{k-1,j})\\&+v^l_{k,j}(h^l_{k,j+1}-h^l_{k,j-1})\\&+\frac{2h^l_{k,j}}{\cos\theta_j}\Bigg[(1-\alpha)(u^l_{k+p/2,j}-u^l_{k-p/2,j})\\&+\frac{\alpha}{2}(u^l_{k+p/2,j+q/2}-u^l_{k-p/2,j+q/2}\\&+u^l_{k+p/2,j-q/2}-u^l_{k-p/2,j-q/2})\Bigg]\frac{1}{p}\\&+\frac{2h^l_{h,j}}{\cos\theta_j}\Bigg[(1-\alpha)(v^l_{k,j+q/2}\cos\theta_{j+q/2}\\&-v^l_{k,j-q/2}\cos\theta_{j-q/2})\end{aligned}$$

$$+\frac{\alpha}{2}\left(v^l_{k+p/2,j+q/2}\cos\theta_{j+q/2}-v^l_{k+p/2,j-q/2}\cos\theta_{j-q/2}\right.$$

$$\left.\left.+\,v_{k-p/2,j+q/2}\cos\theta_{j+q/2}-v_{k-p/2,j-q/2}\cos\theta_{j-q/2}\right)\right]\frac{1}{q}\right\}, \tag{45}$$

where σ is given by (28). If p and q are even integers, the staggered grid does not require any intermediate values. In Fig. 1, we show the location of the grid points used by the unstaggered Turkel–Zwas scheme in each of the equations (for $p = q = 3$). For the staggered grid (again $p = q = 3$) intermediate values are required for h in the momentum equation and for u and v in the continuity equation. It is interesting to see the difference between the staggered grid with $p = q = 2$ and the unstaggered grid with $p = q = 1$. One may feel that if we have $p/2$, $q/2$ instead of p, q respectively, the two above mentioned grids are the same. The truth is that in the momentum equation only h moves closer to the center, and thus the grids are different, see Fig. 2. In the h equation, both u and v move closer to the center and the staggered grid with $p = q = 2$ is now the same as the unstaggered grid with $p = q = 1$, see Fig. 3. Note that the grid for the h equation is identical to that in Fig. 2 and thus not repeated.

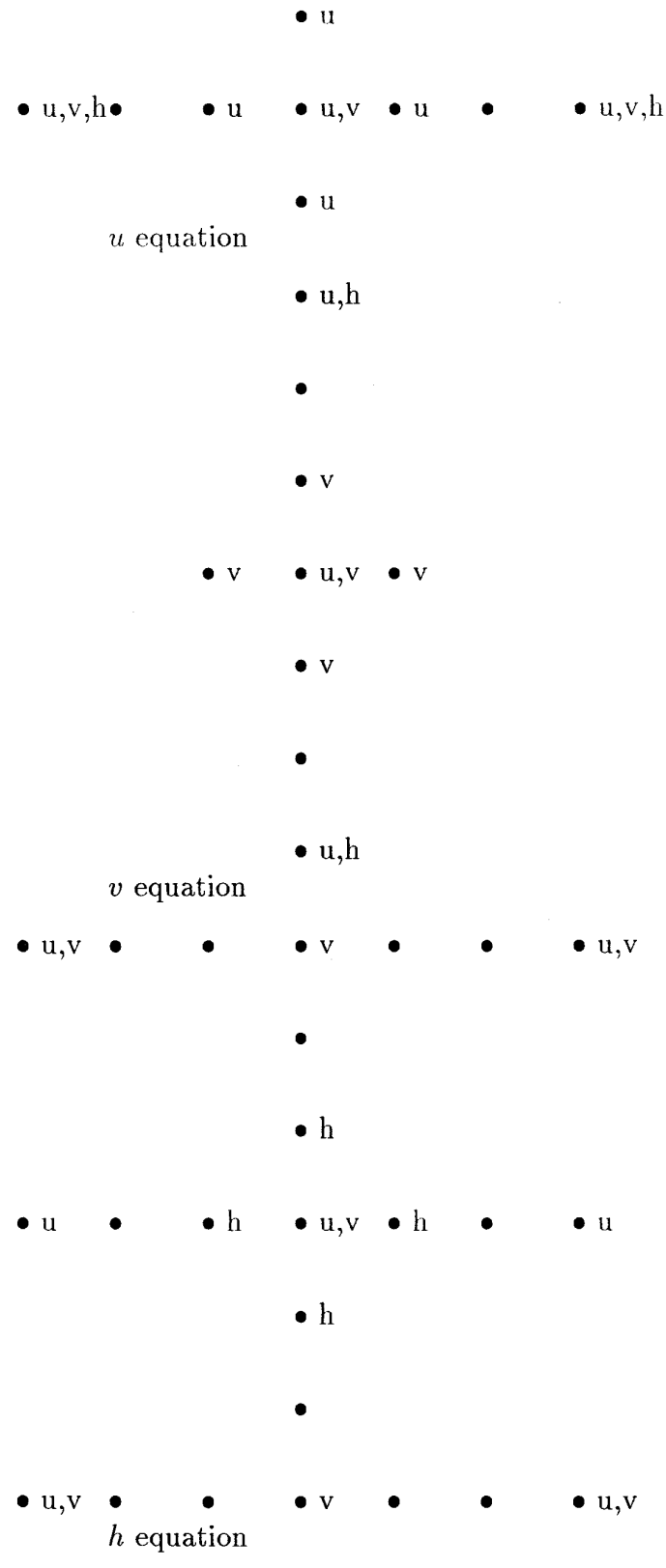

FIG. 1. Unstaggered grid with $p = q = 3$.

4.2. *Modal Expansion for the Staggered System*

We now rewrite (29)–(31) for the staggered grid (semi-discrete staggered Turkel–Zwas scheme)

$$\left.\frac{\partial u}{\partial t}\right|_{k,j}=-\frac{1}{a\,\Delta\lambda}\frac{g}{p\cos\theta_j}\left(h_{k+p/2,j}-h_{k-p/2,j}\right)$$

$$+f_j\left[(1-\alpha)v_{k,j}+\frac{\alpha}{2}\left(v_{k+p,j}+v_{k-p,j}\right)\right] \tag{46}$$

$$\left.\frac{\partial v}{\partial t}\right|_{k,j}=-\frac{1}{a\,\Delta\theta}\frac{g}{q}\left(h_{k,j+q/2}-h_{k,j-q/2}\right)$$

$$-\left[(1-\alpha)f_j u_{k,j}+\frac{\alpha}{2}\left(f_{j+q}u_{k,j+q}+f_{j-q}u_{k,j-q}\right)\right] \tag{47}$$

$$\left.\frac{\partial h}{\partial t}\right|_{k,j}=-\frac{1}{a}\frac{H}{\cos\theta_j}\left[(1-\alpha)\left(\frac{u_{k+p/2,j}-u_{k-p/2,j}}{p\,\Delta\lambda}\right.\right.$$

$$\left.+\frac{v_{k,j+q/2}\cos\theta_{j+q/2}-v_{k,j-q/2}\cos\theta_{j-q/2}}{q\,\Delta\theta}\right)$$

$$+\frac{\alpha}{2}\left(\frac{u_{k+p/2,j+q/2}-u_{k-p/2,j+q/2}}{p\,\Delta\lambda}\right.$$

$$\left.\left.+\frac{u_{k+p/2,j-q/2}-u_{k-p/2,j-q/2}}{p\,\Delta\lambda}\right)\right]$$

$$+\frac{v_{k+p/2,j+q/2}\cos\theta_{j+q/2}-v_{k+p/2,j-q/2}\cos\theta_{j-q/2}}{q\,\Delta\theta}$$

$$+\frac{v_{k-p/2,j+q/2}\cos\theta_{j+q/2}-v_{k-p/2,j-q/2}\cos\theta_{j-q/2}}{q\,\Delta\theta}\Bigg)\Bigg]. \tag{48}$$

Equations (39), (40) are not affected (to second order in $q\,\Delta\theta$) by the staggering. Equation (42) simplifies to

$$\frac{\partial h_{kj}}{\partial t}=-\frac{H}{a}\nabla^2\Phi_{kj}. \tag{49}$$

We seek solutions to (39), (40), and (49) proportional to e^{-ict}, where c denotes the radian frequency. These equations become

$$(\Lambda\nabla^2+i\delta_p)\,\Phi_{kj}+(\mu\nabla^2+\sqrt{1-\mu^2}\,\delta_q)\,i\Psi_{kj}=-i\frac{g}{2a\Omega}\nabla^2h_{kj} \tag{50}$$

$$(\Lambda\nabla^2+i\delta_p)\,\Psi_{kj}-(\mu\nabla^2+\sqrt{1-\mu^2}\,\delta_q)\,i\Phi_{kj}=0 \tag{51}$$

$$h_{kj}=-\frac{Hi}{ac}\nabla^2\Phi_{kj}. \tag{52}$$

Eliminating h_{kj} from (50) by using (52) we have

$$(\Lambda\nabla^2+i\delta_p+\frac{1}{\varepsilon\Lambda}\nabla^4)\,\Phi_{kj}+(\mu\nabla^2+\sqrt{1-\mu^2}\,\delta_q)\,i\Psi_{kj}=0 \tag{53}$$

$$(\mu\nabla^2+\sqrt{1-\mu^2}\,\delta_q)\,i\Phi_{kj}-(\Lambda\nabla^2+i\delta_p)\,\Psi_{kj}=0. \tag{54}$$

Suppose Φ_{kj}, Ψ_{kj} depend on λ_k in the following way,

$$\Phi_{kj}=F_je^{im\lambda_k} \tag{55}$$

$$\Psi_{kj}=G_je^{im\lambda_k}, \tag{56}$$

where m is a nonnegative integer; then

$$\delta_q\Psi_{kj}=\delta_qG_je^{im\lambda_k}=\frac{G_{j+q/2}-G_{j-q/2}}{q\,\Delta\theta}e^{im\lambda_k} \tag{57}$$

$$\delta_p\Phi_{kj}=im\hat{\eta}F_je^{im\lambda_k} \tag{58}$$

and

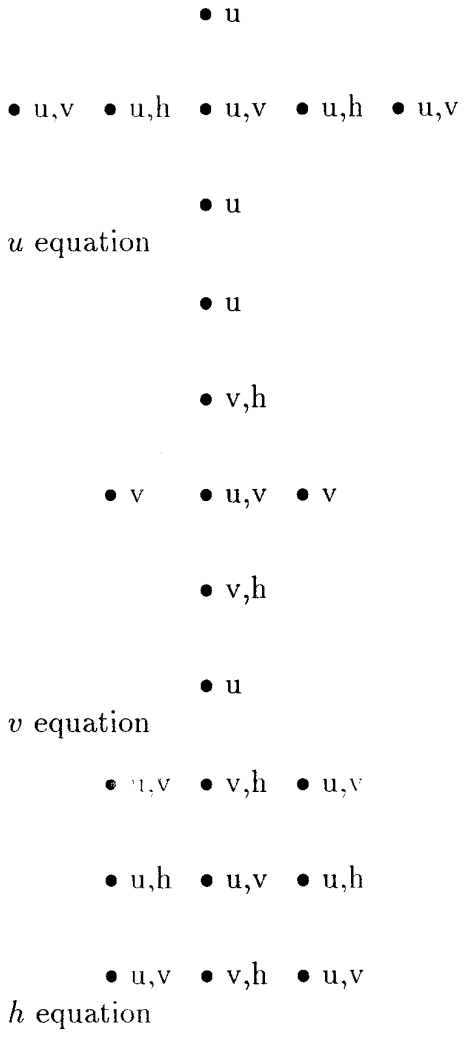

FIG. 2. Staggered grid with $p = q = 2$.

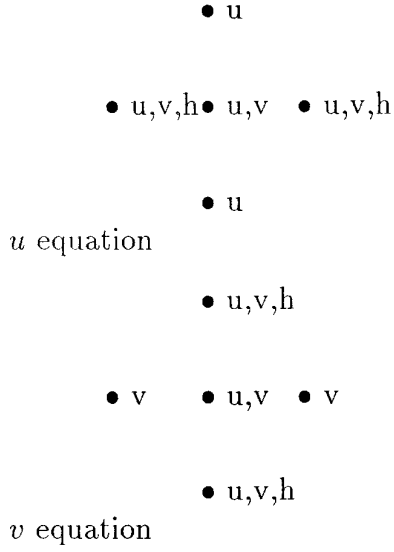

FIG. 3. Unstaggered grid with $p = q = 1$.

$$\nabla^2\Phi_{kj} = \left[\frac{-(m\hat{\eta})^2}{1-\mu^2} + \frac{1}{\sqrt{1-\mu^2}}\,\delta_q(\sqrt{1-\mu^2}\,\delta_q)\right] F_j e^{im\lambda_k}. \tag{59}$$

where

$$\hat{\eta} = \frac{\sin(mp\,\Delta\lambda/2)}{(mp\,\Delta\lambda/2)}.$$

Upon substituting (58) in (53) and (54), we get the semidiscrete analogs of (23) and (19), respectively.

5. COMPARISON OF DISCRETE AND CONTINUOUS MODAL EXPANSIONS

In this section, we compare the equations used for the modal expansion in the continuous case, i.e., (23) and (19), with the corresponding ones for the Turkel–Zwas discretization. These equations for the staggered Turkel–Zwas scheme are (53) and (54), respectively. In the unstaggered case, we were unable to obtain such a system, since (41) is different in form from (13). This difference led us to the development of the staggered scheme.

Note the similarity between (53) and (23). The operator ∇^2, as defined by (21), in (23) is replaced by its discrete analog defined in (36). The operator D, defined by (16), is now discretized by $\sqrt{1-\mu^2}\,\delta_q$. The discrete operator $i\delta_p$ becomes $-m$ in the continuous case. The same analogy holds between (19) and (54).

6. NUMERICAL RESULTS

In this section we present the numerical results for the unstaggered and staggered versions of the Turkel–Zwas scheme. The initial conditions are the same as those used by McDonald and Bates [14], where the height is defined as

$$h(\lambda,\theta,0) = \frac{1}{g}(\overline{\Phi} + 2\Omega a u_o \sin^3\theta\cos\theta\sin\lambda)$$

and the velocities are obtained geostrophically to yield

$$u(\lambda,\theta,0) = -3u_o\sin\theta\cos^2\theta\sin\lambda + u_o\sin^3\theta\sin\lambda$$
$$v(\lambda,\theta,0) = u_o\sin^2\theta\cos\lambda,$$

where

$$g = 9.8\,\frac{\mathrm{m}}{\mathrm{sec}^2}$$

$$\overline{\Phi} = 5.768\times10^4\,\frac{\mathrm{m}^2}{\mathrm{sec}^2}$$

$$u_o = 20\,\frac{\mathrm{m}}{\mathrm{sec}}$$

$$a = 6.370\times10^6\,\mathrm{m}$$

$$\Omega = 7.292\times10^{-5}\,\frac{\mathrm{rad}}{\mathrm{sec}}.$$

The l^2 error norms for the height and velocity are computed in the manner

$$\|h\|_{l^2} = \frac{\sqrt{I[(h(\lambda,\theta)-h_e(\lambda,\theta))^2]}}{\sqrt{I[(h_e(\lambda,\theta))^2]}}$$

and

$$\|\underline{u}\|_{l^2} = \frac{\sqrt{I[(u(\lambda,\theta)-u_e(\lambda,\theta))^2 + (v(\lambda,\theta)-v_e(\lambda,\theta))^2]}}{\sqrt{I[(u_e(\lambda,\theta))^2 + (v_e(\lambda,\theta))^2]}},$$

where

$$I[f(\lambda,\theta)] = \frac{1}{4\pi}\int_0^{2\pi}\int_{-\pi/2}^{\pi/2} f(\lambda,\theta)\cos\theta\,d\theta\,d\lambda.$$

In these relations the variables h_e, u_e, and v_e are considered to be the exact solution. This solution is obtained by a centered in space and time algorithm (a leapfrog scheme) on a 128×64 grid that is time integrated using a time step

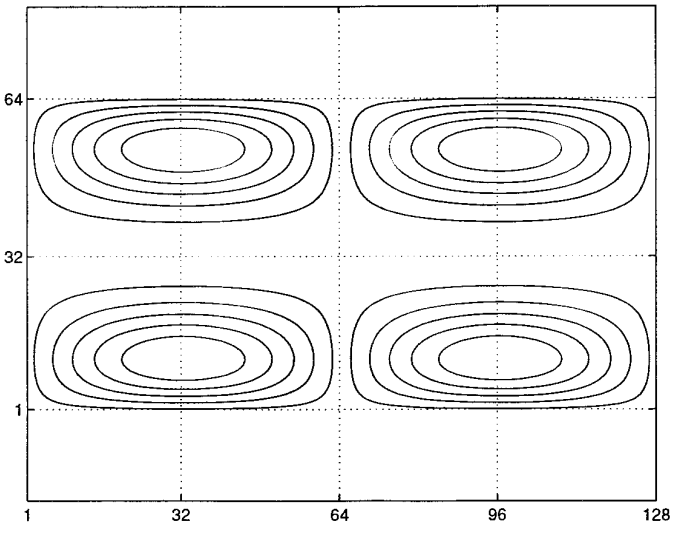

FIG. 4. The height at the initial state ($t = 0$ h). The grid is 128×64.

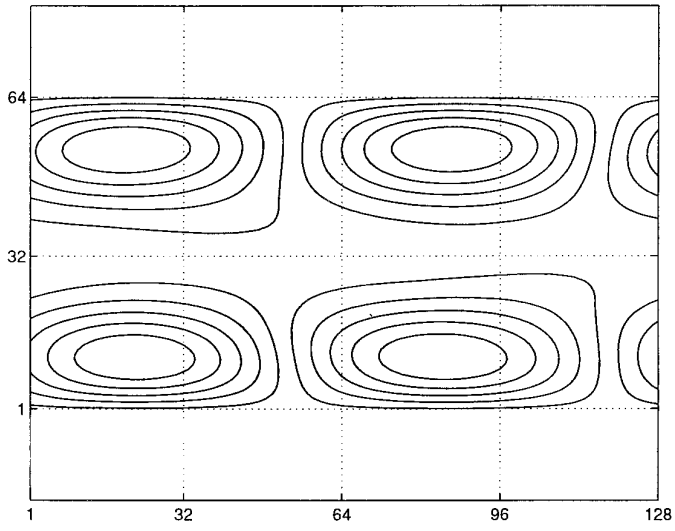

FIG. 5. The height at the final state ($t = 24$ h). The grid is 128×64 and the time step is $\Delta t = 15$ s.

of 15 s. The height at the initial ($t = 0$ h) and final ($t = 24$ h) states is shown in Figs. 4 and 5.

The percentage change in total available energy is defined as

$$\Delta E = \frac{I[E_{final}] - I[E_{initial}]}{I[E_{initial}]} \times 100\%,$$

where

$$E(\lambda, \theta) = \frac{1}{2}\left[h(\lambda, \theta)(u(\lambda, \theta)^2 + v(\lambda, \theta)^2) + \left(h(\lambda, \theta) - \frac{\overline{\Phi}}{g} \right)^2 \right].$$

The shallow water equations are integrated in time for a period of 24 h on a 64×32 grid on a Sparc 10. Table 1 shows the results for various configurations of p and q using different time steps for the unstaggered and staggered versions of the Turkel–Zwas scheme. Recall that p and q refer to the extension of the differencing stencil in the longitudinal (λ) and latitudinal (θ) directions, respectively, and α is the Padé-type differencing weight. We have experimented with various values of α, namely $\alpha = 0, \frac{1}{4}, \frac{1}{3}, \frac{1}{2}, \frac{2}{3}, \frac{3}{4}, 1$. We have found that $\alpha = \frac{1}{3}$ is the best choice. The first row in Table 1 represents the leapfrog scheme, which only allows a time step of 100 s due to the very restrictive CFL condition which limits all explicit algorithms. For the remainder of the cases, p is always greater than q because the time restriction is dictated by the distance between mesh points in the λ direction. As p increases so too does the maximum allowable time step because the CFL restriction is relaxed due to the coarser differencing stencil used for the gravity wave terms. For typical meteorological conditions the inertial gravity wave speeds are larger than the wind velocities while most of the energy is carried by the wind velocities. Thus it makes sense to treat the gravity terms less accurately by using a coarser grid for these terms (see Turkel and Zwas [1]).

TABLE 1

The l^2 Error Norms for the Height h and the Velocity Field u for the Unstaggered and Staggered Versions of the Turkel–Zwas Scheme for a 64×32 Grid after 24 h

Staggered Grid	p	q	α	Δt (s)	$\|h\|_{l^2}$ ($\times 10^{-4}$)	$\|u\|_{l^2}$ ($\times 10^{-3}$)	ΔE (%)	CPU (s)
No	1	1	0	100	1.177	3.722	−0.09	240
No	2	1	1/3	200	1.187	3.830	−0.06	119
No	3	2	1/3	200	2.367	8.018	−0.15	119
Yes	3	2	1/3	200	1.221	4.096	−0.03	119
No	4	2	1/3	200	2.406	8.387	−0.15	119
Yes	4	2	1/3	200	1.269	4.478	0	119
No	3	1	1/3	300	1.193	3.931	−0.06	83
No	5	2	1/3	300	2.475	8.844	−0.15	83
Yes	5	2	1/3	300	1.344	5.081	+0.03	83
No	6	2	1/3	300	2.592	9.471	−0.15	83
Yes	6	2	1/3	300	1.467	5.977	+0.06	83
No	4	1	1/3	400	1.211	4.149	−0.06	61
No	7	2	1/3	400	2.735	10.06	−0.15	61
Yes	7	2	1/3	400	1.634	7.131	+0.09	61
No	8	2	1/3	400	2.881	10.90	−0.15	61
Yes	8	2	1/3	400	1.871	8.585	+0.15	61

Note. The parameter ΔE represents the percentage change of available energy of the system.

Table 1 shows that for lower values of p and q, say ($p = 2, q = 1$) for the unstaggered and ($p = 3, q = 2$) for the staggered and $\Delta t = 200$, the unstaggered and staggered cases yield comparable error norms. As p and q are increased beyond these values, the errors increase dramatically for the unstaggered case; the errors for the staggered case are only half those of the unstaggered case. Note that for the same time step, the staggered case takes no more CPU time than the unstaggered case. In addition, the staggered case where ($p = 4, q = 2$) conserves the total available energy. As p increases, the staggered case no longer conserves the available energy but it is still more accurate than the unstaggered case for the same values of p and q. Therefore for the staggered case the optimal values of p and q must lie somewhere in the vicinity of ($p = 3, q = 2$) and ($p = 4, q = 2$). By comparing the error norms for the unstaggered case for the values ($p = 3, q = 1$) and ($p = 3, q = 2$), and ($p = 4, q = 1$) and ($p = 4, q = 2$), we see that the increase in q from 1 to 2 has adverse effects on the solution accuracy. Therefore it stands to reason that for the staggered case a better solution can be achieved by the values ($p = 3, q = 1$) or ($p = 4, q = 1$). The difficulty with this case is that now interpolation is required because the staggering for odd values of p and q results in intermediate values. Intermediate values in the longitudinal direction pose no difficulty and in fact are handled by linear interpolation in this paper. On the other hand, intermediate values in the latitudinal direction cause problems because interpolation is now required at the poles where the wind velocities are undefined. This case is not included in this paper.

For completeness let us review the case $\Delta t = 200$ once again. The staggered case ($p = 4, q = 2$) yields better results than the unstaggered case ($p = 4, q = 2$). However, the unstaggered case allows a time step of 400 s. The staggered case, on the other hand, cannot use so large a time step because the CFL condition is dictated by terms using the differencing stencil points (p/2, q/2) instead of (p, q). This means that there is a trade-off between computing time and accuracy; for a given value of p and q, the unstaggered case allows a larger time step than the staggered case thereby requiring less CPU time at the cost of lower accuracy. To clarify the point, we recall that Song and Tang have proved that basically the stability condition of the unstaggered case is

$$\frac{\Delta t}{d} = \frac{p}{\sqrt{2gh}}.$$

Since in our case, we have the points half way the original (unstaggered) distance, we replace the numerator by $p/2$, which is the same as halving the value of $\Delta t/d$. For the spherical case, a similar dependence was proved by Turkel and Zwas [1] (see our Introduction).

7. SUMMARY AND CONCLUSIONS

The analysis of the spherical coordinates shallow water equations model shows that the T–Z scheme must be staggered to get eigenvalues and eigenfunctions approaching those of the continuous case. The importance of such an analysis is the fact that it is valid for nonconstant coefficients and thereby applicable to any numerical scheme. In addition, numerical experiments are conducted illustrating the benefits of staggering the original scheme. The numerical experiments show that for given values of p and q the staggered case performs better than the unstaggered case. However, the staggered case requires half the time step of the unstaggered case. This means that there is a trade-off between efficiency and accuracy; for a given value of p and q, the unstaggered case allows a larger time step than the staggered case thereby requiring less CPU time at the cost of lower accuracy. These experiments also show that the best results for the staggered case are obtained with the values ($p = 3, q = 2$) and ($p = 4, q = 2$). Furthermore, the experiments suggest that better results may be obtained by the configurations ($p = 3, q = 1$) and ($p = 4, q = 1$) but interpolation is required in the latitudinal direction because odd values of p or q result in differencing points that do not lie on grid points (intermediate values). Interpolation in the longitudinal direction is straightforward and is handled by linear interpolation in this paper, while in the latitudinal direction it is no longer trivial because intermediate values may fall on the poles where the wind velocities are undefined.

Software for both the unstaggered and staggered Turkel–Zwas schemes for the approximation of the shallow water equations in spherical coordinates is available at URL http://math.nps.navy.mil/~bneta.

ACKNOWLEDGMENTS

This research was conducted for the Office of Naval Research and was funded by the Naval Postgraduate School. The algebraic manipulations were checked by Chris Sagovac using MACSYMA on the VAX at the Electrical and Computer Engineering Department. We are grateful for the referees' and editors' (Dr. J. U. Brackbill, Editor-in-Chief, and Dr. J. K. Dukowicz, Associate Editor) comments, which improved the presentation. The second author (FXG) acknowledges the support of the National Research Council, the Naval Postgraduate School, and the Naval Research Laboratory. The third author (IMN) was partially supported by the Supercomputer Computations Research Institute, which is partially funded by the U.S. Department of Energy through Contract DE-FC05-85ER250000.

REFERENCES

1. E. Turkel and G. Zwas, Explicit large time-step schemes for the shallow water equations, in *Advances in Computer Methods for Partial Differential Equations,* edited by R. Vichnevetsky and R. S. Stepleman (IMACS, Lehigh University, 1979), p. 65.
2. A. L. Schoenstadt, A transfer function analysis of numerical schemes

used to simulate geostrophic adjustment, *Mon. Weather Rev.* **108,** 1248 (1980).

3. B. Neta and I. M. Navon, Analysis for the Turkel–Zwas scheme for the shallow water equations, *J. Comput. Phys.* **81,** 277 (1989).
4. B. Neta and C. L. DeVito, The transfer function analysis of various schemes for the two dimensional shallow water equations, *Comput. Math. App.* **16,** 111 (1988).
5. I. M. Navon and R. deVilliers, The application of the T–Z explicit large time step scheme to a hemispheric barotropic model with constraint restoration, *Mon. Weather Rev.* **115,** 1036 (1987).
6. Navon, I. M., and Yu, J., EXSHALL—A Turkel–Zwas large-time step explicit Fortran program for solving the shallow-water equations on the sphere, *Comput. Geosci.* **17,** 1311 (1991).
7. F. G. Stremler, *Introduction to Communication Systems* (Addison–Wesley, Reading, MA, 1977).
8. J. Steppeler, Analysis of group velocities of various finite element schemes, *Contrib. Atmos. Phys.* **62,** 151 (1989).
9. J. Steppeler, I. M. Navon, and H.-I. Lu, Finite element schemes for extended integration of atmospheric models, *J. Comput. Phys.* **89,** 95 (1990).
10. B. Neta, Analysis of the Turkel-Zwas scheme for the 2-D shallow water equations, in *Transactions on Scientific Computing 1988, Vols. 1.1 and 1.2: Numerical and Applied Mathematics,* edited by W. F. Ames and C. Brezinski (IMACS, 1989).
11. J. Pedlosky, *Geophysical Fluid Dynamics* (Springer-Verlag, New York, 1979).
12. M. S. Longuet-Higgins, The eigenfunctions of Laplace's tidal equations over a sphere, *Phil. Trans. R. Soc. London A* **262,** 511 (1968).
13. Y. Song and T. Tang, On staggered Turkel–Zwas schemes for two-dimensional shallow water equations, *Mon. Weather Rev.* **122,** 223 (1994).
14. A. McDonald and J. R. Bates, Semi-Lagrangian integration of a gridpoint shallow water model on the sphere, *Mon. Weather Rev.* **117,** 130 (1989).